A novel genetic mechanism regulates dorsolateral hinge-point formation during zebrafish cranial neurulation

Molly K. Nyholm[1], Salim Abdelilah-Seyfried[2] and Yevgenya Grinblat[1,*]

[1]Departments of Anatomy and Zoology, University of Wisconsin, Madison, WI 53706, USA
[2]Max Delbrück Center for Molecular Medicine, Robert-Rössle Str. 10, 13125 Berlin, Germany
*Author for correspondence (e-mail: ygrinblat@wisc.edu)

Accepted 19 March 2009
Journal of Cell Science 122, 2137-2148 Published by The Company of Biologists 2009
doi:10.1242/jcs.043471

Summary

During neurulation, vertebrate embryos form a neural tube (NT), the rudiment of the central nervous system. In mammals and birds, a key step in cranial NT morphogenesis is dorsolateral hinge-point (DLHP) bending, which requires an apical actomyosin network. The mechanism of DLHP formation is poorly understood, although several essential genes have been identified, among them *Zic2*, which encodes a zinc-finger transcription factor. We found that DLHP formation in the zebrafish midbrain also requires actomyosin and Zic function. Given this conservation, we used the zebrafish to study how genes encoding Zic proteins regulate DLHP formation. We demonstrate that the ventral *zic2a* expression border predicts DLHP position. Using morpholino (MO) knockdown, we show *zic2a* and *zic5* are required for apical F-actin and active myosin II localization and junction integrity. Furthermore, myosin II activity can function upstream of junction integrity during DLHP formation, and canonical Wnt signaling, an activator of zic gene transcription, is necessary for apical active myosin II localization, junction integrity and DLHP formation. We conclude that zic genes act downstream of Wnt signaling to control cytoskeletal organization, and possibly adhesion, during neurulation. This study identifies *zic2a* and *zic5* as crucial players in the genetic network linking patterned gene expression to morphogenetic changes during neurulation, and strengthens the utility of the zebrafish midbrain as a NT morphogenesis model.

Supplementary material available online at
http://jcs.biologists.org/cgi/content/full/122/12/2137/DC1

Key words: Zic, Dorsolateral hinge point, Actomyosin, Wnt

Introduction

Neurulation is the major morphogenetic process that shapes the vertebrate central nervous system (CNS, the future brain and spinal cord) during embryonic development. Disruptions in normal neurulation result in neural tube defects (NTDs), including closure defects in the brain (exencephaly), trunk (spina bifida), or both (craniorachischisis). NTDs are widespread, affecting 1 or 2 per 1000 human births (Copp et al., 2003). Given the serious and prevalent nature of NTDs, it is essential that we understand the complex molecular and genetic basis of neurulation. Mutant and knockdown analyses have begun to identify genes and molecules important for each step in neurulation, and suggest that several coordinated cellular processes including actomyosin contraction, intercellular adhesion, proliferation, and convergence and extension (CE) are required for NT closure.

Vertebrates use different strategies to complete neurulation. This study focuses on cranial neurulation, which, in mammals and birds, follows a process termed primary neurulation. Following neural induction, the cranial neural plate thickens at the lateral edges to form neural folds. These folds elevate toward the dorsal surface and bend inward toward the dorsal midline at dorsolateral hinge points (DLHPs). Finally, the two folds fuse dorsally to close the NT (Colas and Schoenwolf, 2001; Morriss-Kay et al., 1994; Smith and Schoenwolf, 1997). In zebrafish, a teleost, neural plate cells elongate and converge to form a neural keel, and then intercalate to form a dorsally closed rod (Hong and Brewster, 2006). This solid rod subsequently forms DLHPs and cavitates to make a tube (Fig. 1A). Although DLHPs form after NT closure in zebrafish, they appear to be important for lumen shape and might be controlled by the same molecular mechanisms that regulate DLHP formation in mammals and birds.

Analyses of mouse mutants demonstrate that the majority of cranial NTDs involve disruption in DLHPs (Copp, 2005). A contractile actomyosin network at the apical neuroepithelial surface provides a critical force in DLHP bending and NT closure. Indeed, microfilaments localize subapically in neuroepithelial cells during bending (Sadler et al., 1982; van Straaten et al., 2002). Mutations in mouse *p190 RhoGAP* (Brouns et al., 2000), *Shroom* (Hildebrand, 2005; Hildebrand and Soriano, 1999), *Mena and Profilin* (Lanier et al., 1999) or *Mena* and *VASP* (Menzies et al., 2004), which encode proteins with actin-related functions, cause exencephaly. Knockdown of Shroom3 (Haigo et al., 2003; Lee et al., 2007) or Xena (Roffers-Agarwal et al., 2008) in *Xenopus* similarly causes NT closure defects through misregulation of the actin cytoskeleton. Moreover, inhibition or activation of Rho, a regulator of the cytoskeleton, prevents normal apical Rho accumulation and NT closure in the chick (Kinoshita et al., 2008). The requirement for actomyosin contraction in DLHP bending is further supported by experiments designed to disrupt the actomyosin network pharmacologically. Cytochalasin D, which disrupts actin polymerization, and blebbistatin, which inhibits myosin II, can both prevent DLHP formation and cause cranial NTDs in the chick (Kinoshita et al., 2008; Morriss-Kay and Tuckett, 1985; Schoenwolf et al., 1988). Interestingly, neurulation in the trunk is not as sensitive

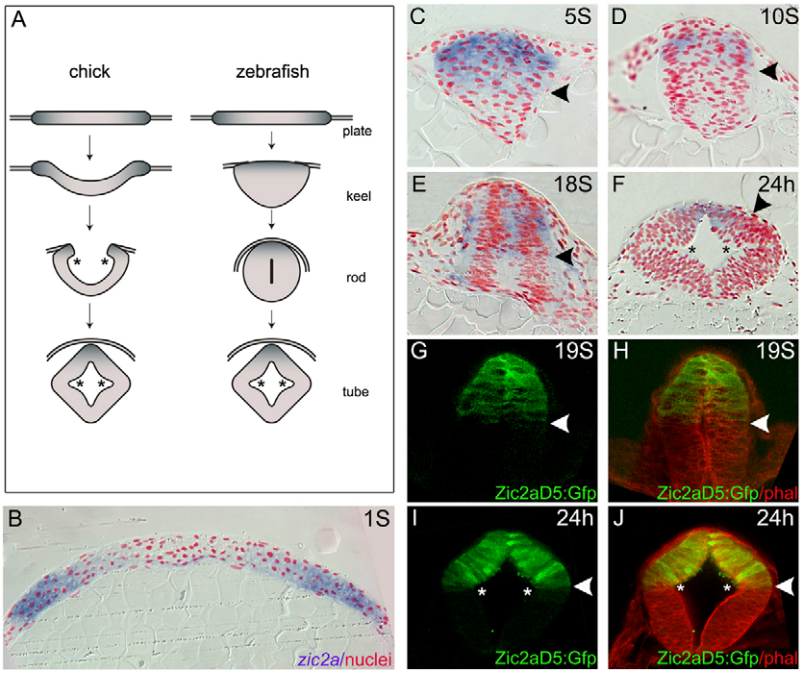

Fig. 1. *zic2a* expression during zebrafish midbrain neurulation. (A) Schematic comparison between chick and zebrafish cranial neurulation. Presumptive dorsal tissue is shaded more darkly than ventral. DLHPs (asterisks) form before NT closure in chick, but after closure in zebrafish. (B-F) Wild-type zebrafish embryos stained at indicated stages for *zic2a* (purple) and for nuclei (red) by ISH with Neutral red. Ventral Zic expression border is labeled with black arrowheads. DLHPs form between 18-somite (18S) stage and 24 hpf. (G-J) *Tg(zic2a-D5:egfp)* embryos showing expression of GFP (green). (H,J) Phalloidin (red) counterstain. DLHPs (asterisks) form at the ventral border of GFP expression (white arrowheads). Images show midbrain cross-sections, dorsal at the top. Embryonic stages are listed in upper right corners.

to cytoskeletal changes, suggesting that the role for microfilaments may be cranial specific (Ybot-Gonzalez and Copp, 1999).

Apical actomyosin is intimately linked to apical junctions, which establish apicobasal polarity and cell-cell adhesion. Non-muscle myosin II activity is required for junction remodeling in *Drosophila* and in cell culture (Bertet et al., 2004; Kishikawa et al., 2008; Miyake et al., 2006; Zallen and Wieschaus, 2004). An interaction between actomyosin and apical junctions is also important during neurulation. For example, mutations in the gene encoding vinculin, which links F-actin to adherens junctions, result in exencephaly in mouse (Xu et al., 1998). Furthermore, mutations in junction components themselves disrupt neurulation. Mutations in the gene encoding N-cadherin, a component of adherens junctions, cause NTDs in zebrafish, and disruptions of tight junction components such as *mpp5a/nok*, disturb zebrafish NT morphogenesis (Bit-Avragim et al., 2008; Hong and Brewster, 2006; Lowery and Sive, 2005).

Conflicting evidence exists on the importance of cell proliferation in neurulation. Chemically blocking the cell cycle does not affect neurulation in zebrafish or *Xenopus* (Ciruna et al., 2006; Harris and Hartenstein, 1991; Lowery and Sive, 2005), yet many exencephalic mouse mutants display changes in proliferation. Either upregulation or downregulation of proliferation can be correlated with exencephaly in mice. Mutations in tumor suppressor genes such as *p53* and *Brca1* can lead to excessive growth and exencephaly (Gowen et al., 1996; Sah et al., 1995), whereas mutations in neuronal differentiation genes such as *Hes* and *Numb* can cause premature differentiation, reduced proliferation and cranial NTDs (Ishibashi et al., 1995; Zhong et al., 2000). Recent studies in mouse suggest a variation in proliferation rates along the dorsoventral (D-V) axis might be important. Mutations in *Phactr4*, a PP1 kinase cause an increase in proliferating cells in the ventral neural tube, thereby disrupting a D-V proliferation gradient and resulting in exencephaly (Kim et al., 2007).

Convergence and extension (CE) are responsible for narrowing and lengthening the neuroepithelium during neurulation (Kibar et al., 2007). CE is controlled by the non-canonical Wnt pathway, the vertebrate equivalent of the *Drosophila* PCP pathway (Wang and Nathans, 2007). In mice, mutations in PCP genes (e.g. *Celsr3*, *Dvl1*, *Dvl2*, *CthrC1* and *Vangl2*) disrupt CE and result in a wide neural plate with neural folds that are too far apart to close (Curtin et al., 2003; Wang et al., 2006; Yamamoto et al., 2008; Ybot-Gonzalez et al., 2007b). Zebrafish with compromised *vangl2*, *prickle* or *wnt11* function also have neurulation defects, suggesting that this role of PCP is conserved (Ciruna et al., 2006; Jessen et al., 2002; Tawk et al., 2007; Veeman et al., 2003).

Zic genes encode a family of zinc-finger transcription factors that are required for NT closure and cell-cycle regulation in mammals (Aruga et al., 1996; Merzdorf, 2007). Specifically, mutations in *Zic2* and *Zic5* cause exencephaly and spina bifida in mouse and humans (Elms et al., 2003; Grinberg and Millen, 2005; Inoue et al., 2004; Nagai et al., 1997). Recent *Zic2* loss-of-function studies in mouse indicate these defects may result from a failure in DLHP formation, at least in the posterior spinal cord (Ybot-Gonzalez et al., 2007a). Zic proteins have been described as cell-cycle regulators that maintain cells in a proliferative state and prevent differentiation (Aruga et al., 2002; Brewster et al., 1998; Ebert et al., 2003; Nyholm et al., 2007). Whether Zic proteins regulate proliferation independently of their role in morphogenesis, or whether the two functions are interdependent, is unknown.

In this study, we exploit the zebrafish model to further elucidate the mechanisms of zic gene function during neurulation. The zebrafish zic genes are organized as linked pairs in the genome. We focused on one pair, *zic2a* and *zic5*, because their mammalian homologs have a documented role in neurulation, and because we previously showed that they are co-regulated and have overlapping expression patterns and functions in the midbrain (Nyholm et al., 2007). On the basis of the expression patterns of these two zic genes and results of knockdown assays, we show a conserved requirement for *zic2a* and *zic5* in zebrafish cranial neurulation, specifically in DLHP bending. We demonstrate that zic genes are not essential for CE or PCP, but have a key role in controlling

apical actomyosin and junction integrity during DLHP formation. Furthermore, we show that blocking cell proliferation does not impair myosin II activity, junction integrity, or DLHP formation during zebrafish neurulation. When combined with previous studies, our data suggest zic genes act downstream of canonical Wnt signaling to regulate cytoskeletal organization independently of their role in proliferation.

Results

zic gene expression correlates with DLHP formation

To test whether conserved genetic mechanisms regulate DLHP formation in zebrafish, we investigated whether zebrafish *zic2a* or *zic5* are involved in DLHP development. We first mapped *zic2a* and *zic5* expression domains relative to DLHP in cross-sections through the midbrain (Fig. 1). At the end of gastrulation, *zic2a* was transcribed at the lateral edges of the neural plate, the future dorsal NT (purple, Fig. 1B). During neural keel and rod stages (5-18 somite), *zic2a* RNA continued to be dorsally restricted (Fig. 1C-E). The ventral limit of expression appeared to correlate with the future location of DLHPs. By 24 hpf, when the lumen and DLHPs were formed, the ventral limit of *zic2a* expression shifted and was found dorsal to DLHPs (Fig. 1F). *zic5* RNA was distributed similarly (not shown).

To see whether the ventral *zic2a* and *zic5* expression border in the neural rod coincided with DLHPs, we used *Tg(zic2a-D5:egfp)* embryos that express GFP under *zic2a* promoter control (Nyholm et al., 2007). *Tg(zic2a-D5:egfp)* embryos were labeled with phalloidin, a marker of F-actin, to outline cells and examined in cross-section through the midbrain. At the 19-somite stage, GFP distribution resembled that of the *zic2a* and *zic5* RNA, ending just where DLHPs were initiating (Fig. 1G,H). At 24 hpf, the GFP expression border precisely marked the location of fully formed DLHPs (Fig. 1I,J). GFP was distributed differently from endogenous *zic2a* and *zic5* RNA, probably because of the long half-life of GFP protein. These data demonstrate that the ventral limit of *zic2a* and *zic5* expression in the neural rod precisely coincides with the future DLHP position.

zic2a and *zic5* are required for DLHP formation

The striking correlation between the *zic2a* and *zic5* expression border and DLHPs suggested that these zebrafish genes might have a role in DLHP formation. We have previously documented ventricle inflation and shape defects in embryos with compromised *zic2a* and *zic5* function (Nyholm et al., 2007). This defect is not due to cell death because no increase in apoptosis is observed in zic morphants (Nyholm et al., 2007) and co-injecting a p53 morpholino along with the zic morpholinos fails to rescue the morphant defect (supplementary material Fig. S1). We hypothesized that zic (*zic2a* and *zic5*) morphant ventricle defects might result from a failure in HP formation. Midbrain morphology was examined in cross-section through morphants at 21-somite stage and 24 hpf. At the 21-somite stage, DLHPs were initiated normally in embryos injected with standard control morpholino (conMO) (Fig. 2A, *n*=2), but did not form in embryos injected with *zic2a* and *zic5* splice-blocking morpholinos (Fig. 2B, *n*=5). By 24 hpf, DLHPs were well defined in controls (asterisks, Fig. 2F, *n*=3) and absent in zic morphants (Fig. 2G,H, *n*=9/9). Hinge points were also missing in embryos injected with a combination of two morpholinos designed to block translation of *zic2a* mRNA (supplementary material Fig. S1, *n*=4/4). Among the morphants, some had small lumens with little or no HP bending (Fig. 2G, *n*=8/13), whereas others had open lumens but little HP bending (Fig. 2H, *n*=5/13). Since morphants can inflate ventricles without DLHPs, this suggests that DLHP bending is not required for lumen opening, but rather for the overall shape of the NT. In other words, lumen inflation and HP formation appear to be separable. Together, the *zic2a* and *zic5* expression pattern and absence of DLHPs in morphants suggest that these zic genes are required for DLHP formation and are part of a conserved genetic mechanism for DLHP formation in vertebrates.

Myosin II activity is required for zebrafish DLHP formation

In addition to zic genes, several genes important for DLHP formation are involved in actomyosin function (Copp, 2005). To test whether actomyosin is required for zebrafish DLHP development, we inhibited actomyosin contraction by treating neural rod (15- to 16-somite-stage) embryos with blebbistatin, a small molecule inhibitor of myosin II (Kovacs et al., 2004). Following treatment, midbrain cross-sections were examined for the presence of DLHPs at the 21-somite stage and 24 hpf. DMSO-treated controls (Fig. 2D, *n*=4) or controls treated with an inactive enantiomer of blebbistatin (not shown, *n*=2) were just beginning to form DLHPs and had a small lumen at the 21-somite stage, whereas blebbistatin-treated embryos showed no evidence of a lumen or DLHPs (Fig. 2E, *n*=5). By 24 hpf, controls treated with DMSO (Fig. 2I, *n*=4) or inactive blebbistatin (not shown, *n*=2) had well-defined HPs (asterisks) and a diamond-shaped lumen. Blebbistatin-treated embryos failed to form HPs and had little or no lumen (Fig. 2J, *n*=6). Similar ventricle (lumen) defects were observed in embryos treated with ML7, a myosin light chain kinase inhibitor; however, this treatment also caused progressive and widespread cell death (data not shown). These results show a requirement for myosin II activity in zebrafish cranial neural tube

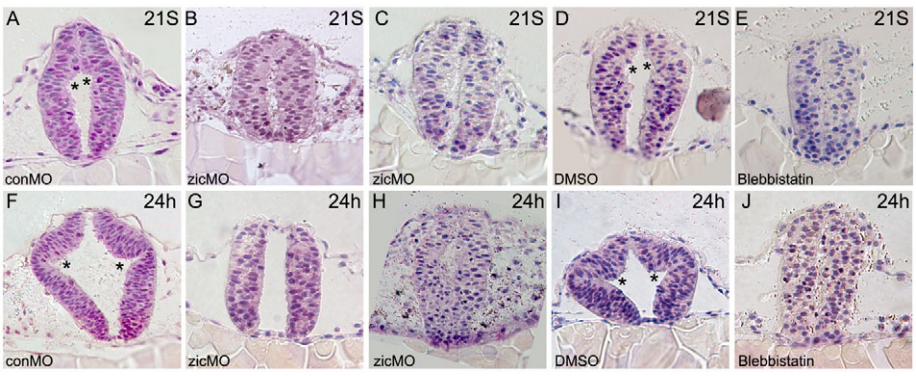

Fig. 2. *zic2a*, *zic5* and actomyosin contraction are required for DLHP formation. Cross-sections through zebrafish midbrains stained with hematoxylin (purple) to label nuclei at 21-somite stage (A-E) and 24 hpf (F-J). (A) Control morphants show initial DLHP bending (asterisks). (B,C) The zic morphants have a small central lumen, but no DLHPs. (D) DMSO-treated controls display initial DLHP bending. (E) Blebbistatin-treated embryo with no DLHPs. (F) Control morphants have fully developed DLHPs. (G,H) The zic morphants show either an open lumen with no DLHPs (G) or a small lumen with very little DLHP bending (H). (I) DMSO controls form normal DLHPs. (J) Blebbistatin treatment inhibits DLHPs and prevents lumen opening.

morphogenesis, particularly in DLHP formation, and suggest that actomyosin contraction is a conserved aspect of DLHP development in zebrafish.

zics regulate apical F-actin and active myosin II

Because zic morphants and blebbistatin-treated embryos both fail to form DLHPs, we hypothesized that zic gene expression might be necessary for apical actomyosin contraction. To test this, we labeled actin filaments (F-actin) with phalloidin and active myosin II filaments with anti-phosphorylated regulatory myosin light chain (anti-rMLC-*P*). Anti-rMLC-*P* detects phosphorylation of myosin II regulatory light chains on Ser19, which is required for actin to activate myosin II, and has been used as an indicator of active actomyosin contraction (Koppen et al., 2006; Lee et al., 2006; Somlyo and Somlyo, 2003). At the 16-somite stage, before DLHP formation begins, F-actin and rMLC-*P* were concentrated apically in the dorsal midbrain, i.e. at the future luminal surface, in controls (Fig. 3A-C, *n*=6), but showed no apical enrichment in zic morphants (Fig. 3D-F, *n*=4/6). By the 19-somite stage, apical F-actin (*n*=22) and rMLC-*P* (*n*=4) were restricted to a narrow, contiguous domain (an apical seam) in controls (Fig. 3G-I). Morphants displayed patches of apical staining at 19-somite stage, but failed to form a contiguous seam of actomyosin (Fig. 3J-L, *n*=5/5 rMLC-*P* and phalloidin, *n*=24/28 phalloidin alone). Cross-sections through phalloidin-stained *Tg(zic2a-D5:EGFP)* embryos established that F-actin was most disorganized dorsally, within the zic expression domain, in morphants (Fig. 3M-O compared with Fig. 3P-R). Quantitative analysis showed that apical F-actin levels were significantly reduced in zic morphants (Fig. 3S-T). rMLC-*P* was similarly disrupted dorsally, but not ventrally (supplementary material Fig. S2).

We further confirmed the actomyosin defect in zic morphants using live imaging in embryos transiently expressing mCherry fused to the actin-binding domain of Utrophin (mCherry-Utr-CH). This Utr-CH probe reliably labels F-actin in living cells (Burkel et al., 2007). Time-lapse analysis from 14-somite to 18-somite stages demonstrated that wild-type and control morphant embryos assembled a well-defined apical F-actin seam by ~17-somite stage, and maintained this seam for the duration of the experiment (supplementary material Fig. S3 and Movie 1; *n*=3). By contrast, zic morphants showed disorganized F-actin distribution throughout the experiment (supplementary material Fig. S3 and Movie 2; *n*=3).

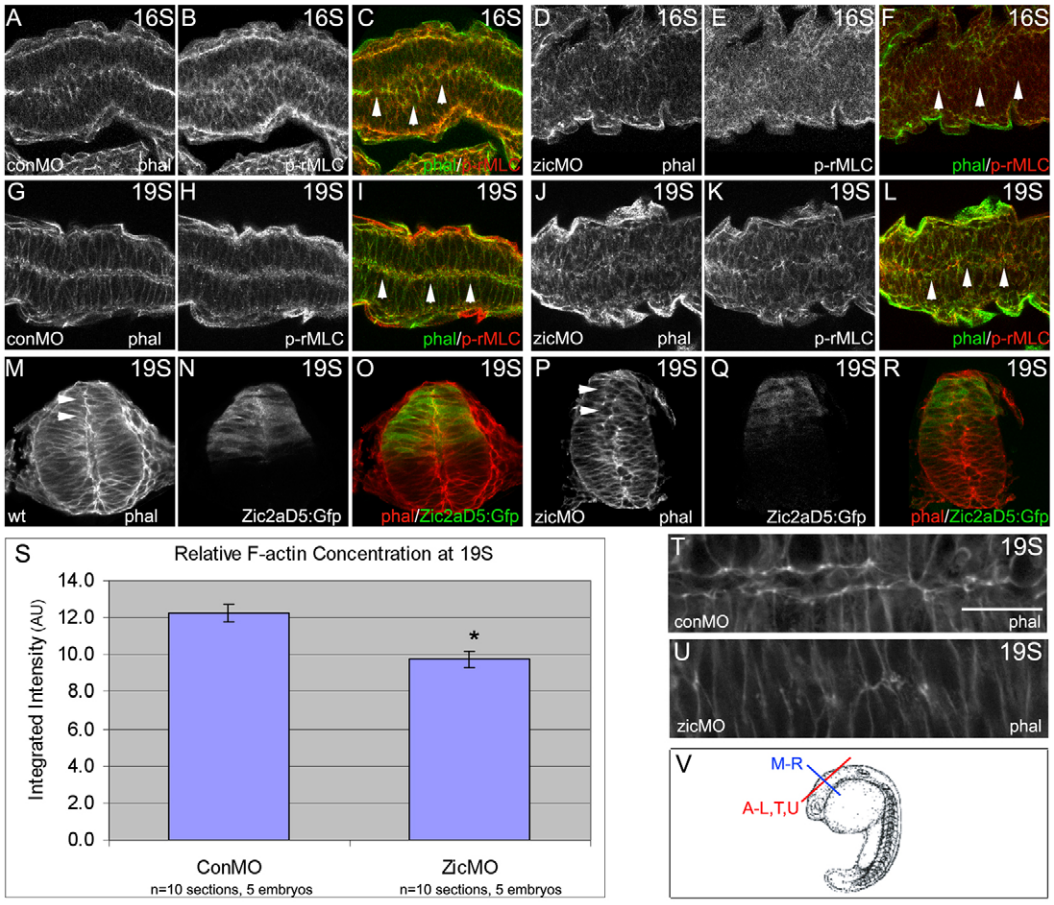

Fig. 3. *zic2a* and *zic5* are required for apical F-actin localization and phosphorylated-myosin-II expression. (A-L) Horizontal sections through dorsal midbrain, anterior on the left, showing phalloidin (green) and rMLC-*P* (red) expression. At 16-somite stage, broad apical staining is seen in controls (A-C), but not zic morphants (D-F). By the 19-somite stage, a tight apical seam of staining is apparent in controls (G-I), but not in morphants (J-L). (M-R) Midbrain cross-sections, dorsal at the top, of *Tg(zic2a-D5:egfp)* embryos showing GFP (green) and phalloidin (red). (M-O) Controls show a contiguous apical seam of F-actin. (P-R) The zic morphants display disorganized phalloidin staining, particularly within the GFP domain. (C,I,O,F,L,R) Colored overlays of the images to the left. (S) 19-somite-stage zic morphants contain significantly less F-actin (*P<0.002) in the apical region than control morphants, based on measurements from high-magnification phalloidin-stained images. Error bars represent s.e.m. Representative images used for these measurements are shown in T (control morphant) and U (zic morphant). Scale bar: 20 μm. (V) Approximate location of the sections shown above. Arrowheads indicate the apical seam in C-L and dorsal apical seam in M and P.

Together, fixed and live analyses suggest that DLHP failure in zic morphants results from a defect in cytoskeletal organization and a lack of apical actomyosin contraction, and place Zics functionally upstream of actomyosin contraction in the dorsal neuroepithelium.

zic2a and *zic5* are required for apical junction integrity

Because actomyosin is associated with apical junctions, actomyosin defects in zic morphants might be due to defective apical junctions in the neuroepithelium. To test this, we examined expression of three apical junction markers in zic morphants. First, we used an antibody against β-catenin, an armadillo repeat protein that controls cadherin-mediated adhesion, to label adherens junctions (Brembeck et al., 2006; Tepass et al., 2000). β-catenin was apically enriched in wild-type midbrains at the 19-somite stage (Fig. 4A,C, *n*=5). The zic morphants displayed patchy β-catenin staining in the dorsal midbrain and more contiguous β-catenin staining ventrally (Fig. 4B,D, *n*=9). Next, we used a membrane protein, palmitoylated 5a (Mpp5a) as an indicator of tight junctions. Mpp5a is a MAGUK family scaffolding protein that functions as part of the Crumbs complex, and is required for maintenance of cell polarity and epithelial integrity in the NT (Bit-Avragim et al., 2008; Wei and Malicki, 2002). Mpp5a localized in an apical seam throughout the midbrain of controls at the 19-somite stage (Fig. 4E,F, *n*=7). Morphants displayed irregular apical Mpp5a distribution in the dorsal midbrain, but normal protein in the ventral midbrain (Fig. 4G,H, *n*=3).

Finally, we used another MAGUK family protein, ZO-1, as an apical junction marker. ZO-1 associates with tight junctions in mature neuroepithelia, but can associate with adherens junctions in developing epithelia (Aaku-Saraste et al., 1996; Itoh et al., 1993). At the 16-somite stage, ZO-1 labeled an apical seam in controls, and this seam was patchy in zic morphants (not shown, *n*=4 controls, 4 of 5 morphants). In 19-somite controls anti-ZO-1 labeled two apical domains on either side of the neuroepithelium (Fig. 4I,K,M, *n*=6). In the dorsal midbrain of morphants, ZO-1 was patchy and failed to separate into two apical domains (Fig. 4J,N, *n*=14). At 24 hpf ZO-1 and F-actin distribution was similarly affected in morphants that developed without a lumen and those that formed small lumens (supplementary material Fig. S4). Consistently with the other apical markers, ZO-1 appeared unaffected in the ventral midbrain (Fig. 4L). In summary, all three apical markers examined were somewhat disrupted in the morphant dorsal midbrain, but still found predominantly at or near the apical cell surface. These data suggest that Zic proteins are required to establish and/or maintain apical junctions.

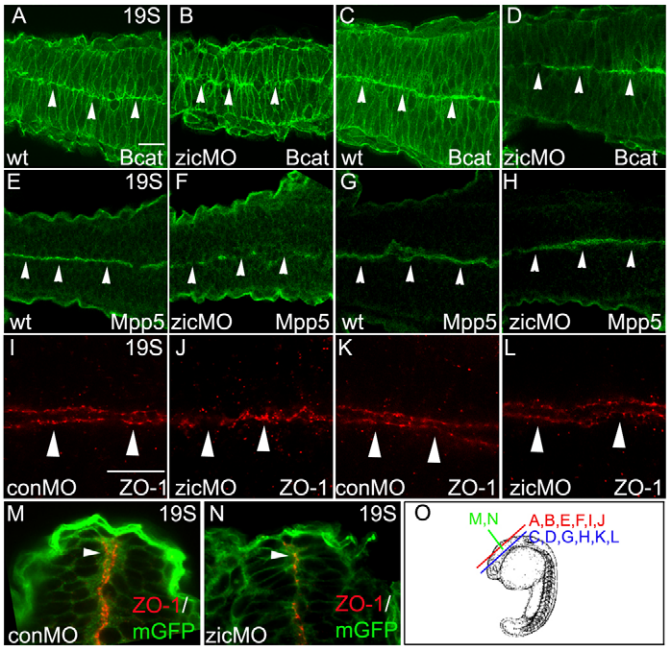

Fig. 4. Expression of apical junction markers in zic morphants. (A-L) Horizontal confocal sections through midbrain of immunolabeled embryos at 19-somite stage; anterior is on the left. (A-D) β-Catenin localizes to a contiguous apical domain in wild-type embryos (A,C). Apical β-catenin is patchy and discontinuous at the dorsal apical surface in zic morphants (B), but appears unaffected ventrally (D). Similar patterns are seen with Mpp5 (E-H) and ZO-1 (I-L). (M-N) Cross-sections through dorsal midbrain showing ZO-1 (red) and membrane-targeted mGFP (green) in controls (M) and zic morphants (N). (O) Approximate locations of the sections shown above.

zic2a and *zic5* regulate DLHPs independently of planar polarity

In addition to apical-basal polarity, neuroepithelial cells also have planar polarity. Although zic morphants do not show a CE defect during gastrulation (not shown), a later planar polarity defect could contribute to the phenotype we described in the neuroepithelium. We assessed planar polarity in zic morphants using two previously published methods. First, since components of the PCP pathway regulate orientation of cell division (Gong et al., 2004), we asked whether dividing cells were properly oriented in the neural rod. The angle of cell division, i.e. the angle between the mitotic spindle axis and the midline, was measured in horizontal sections through the dorsal midbrain of 15-somite *Tg(pBOS:H2Bgfp)* embryos (see Materials and Methods) (Fig. 5A,B). Consistent with published studies, more than 85% of the wild-type cells divided within a 80-120 degree angle relative to the midline in controls (Geldmacher-Voss et al., 2003) (Fig. 5C, *n*=38 cells in 4 embryos). In morphants, anaphase cells were similarly oriented relative to the midline (*n*=35 cells in 5 embryos), suggesting that the midline-crossing orientation of division is unaffected in morphants.

As a second measure of planar polarity, we used anterior membrane localization of GFP-Pk, which has been used as a read-out of PCP in the spinal cord and notochord at neural keel stages (Ciruna et al., 2006). In controls 70.5% of GFP-Pk-expressing cells showed punctate distribution, and 39.3% of cells showed puncta at the anterior membrane. In morphants, 64.1% of expressing cells displayed punctate distribution, and 41% showed anteriorly biased puncta at the 12-somite stage (Fig. 5D-F) (*n*=61 cells in 6 controls and *n*=39 cells in 5 morphants). Together, these two assays indicate that planar polarity is established normally in zic morphants. We therefore concluded that zic gene expression is not necessary for PCP or non-canonical Wnt signaling during neurulation.

zic2a and *zic5* are required for cell-cycle progression

In addition to actomyosin contraction and planar polarity, controlled rates of proliferation are important for NT morphogenesis in mammals (Gowen et al., 1996; Ishibashi et al., 1995; Kim et al., 2007; Sah et al., 1995; Zhong et al., 2000). We previously observed a reduction in M-phase cells in zic morphants (Nyholm et al., 2007). To investigate whether the cytoskeletal organization defects described above may be caused by reduced proliferation, we analyzed the timing of the cell-cycle defect in zic morphants. To analyze the S phase, embryos were exposed to BrdU at 16-somite

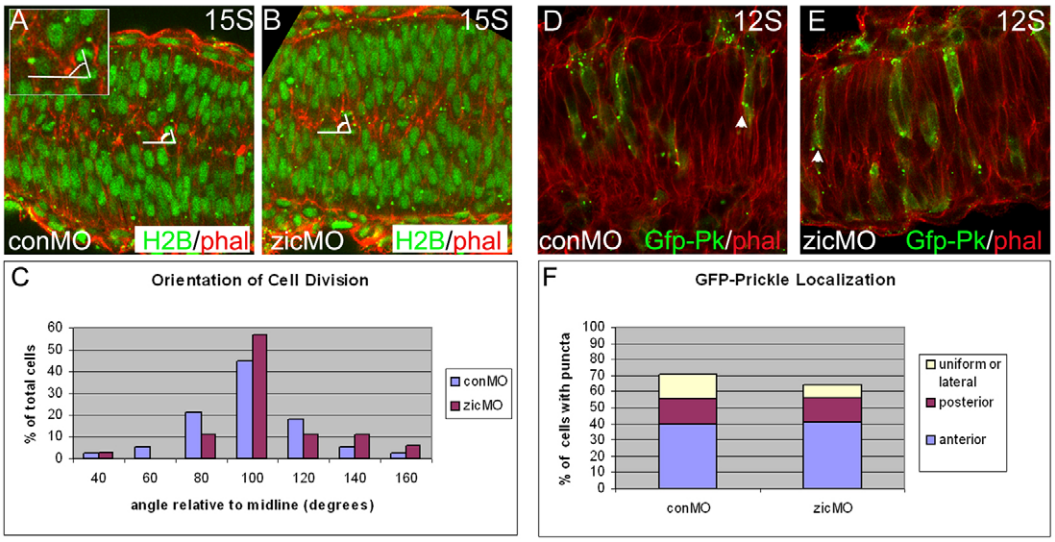

Fig. 5. Division orientation and GFP-Pk localization are normal in zic morphants. (A,B) Horizontal sections, anterior to the left, of 15-somite-stage embryos labeled with Histone2B:GFP (green) and phalloidin (red). Control (A) and zic morphant (B) embryos both show normal midline-crossing divisions. Lines drawn parallel to the midline and between anaphase chromosomes (white lines) were used to measure division orientation (inset in A). (C) Morphants and controls show comparable distributions of division angles, with the majority of cells dividing 80-120 degrees relative to the midline. (D-E) Horizontal sections, anterior to the left, of 12-somite-stage embryos scatter-labeled with GFP-Pk (green) and counterstained with phalloidin (red). Controls (D) and morphants (E) show cells with anteriorly biased GFP-Pk membrane puncta (arrowheads). (F) A comparison of GFP-Pk localization in controls and morphants.

or 18-somite stage and immediately fixed for immunodetection of BrdU. To test for D-V-restricted effects, the proportion of BrdU-positive cells was calculated within three separate regions: the dorsal, middle, and ventral thirds of each midbrain cross-section. The proportion of S-phase cells was not statistically different between morphants and controls at 16-somite stage in any D-V region (Fig. 6A). By the 18-somite stage, however, zic morphants had significantly fewer S-phase cells in both the dorsal (P<0.002) and ventral (P<0.008) regions when compared with controls using the Student's t-test (Fig. 6B-D). Given that the ventral reduction we see in morphants is outside the *zic2a* and *zic5* expression domain, it is probably a secondary effect of Zic depletion dorsally. These data are consistent with the moderate reduction in M-phase cells that we saw at the 16-somite stage (not shown, n=5 controls and 6 morphants) and the previously reported significant drop in M-phase cells by the 19-somite stage (Nyholm et al., 2007), and allow us to

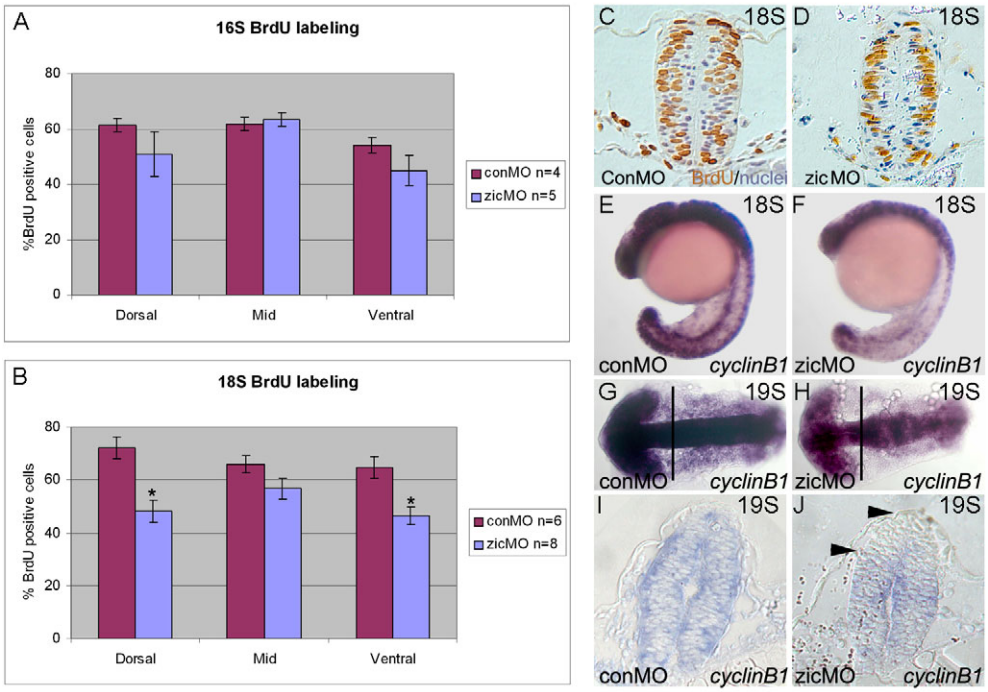

Fig. 6. The zic morphants have fewer S-phase cells and reduced *ccnb1* transcript levels in the dorsal midbrain. (A) The percentage of BrdU-positive cells is not significantly reduced in zic morphants at 16-somite stage. (B) At 18-somite stage, zic morphants contain significantly fewer BrdU-positive cells in the dorsal midbrain (*P<0.002) and ventral midbrain (*P<0.008), determined by Student's t-test. To further investigate whether the number of S-phase cells was different across the dorsoventral axis for controls and zic morphants, we performed ANOVA analysis and found no significant difference (P=0.320). Error bars represent s.e.m. (C-D) Representative midbrain sections stained with anti-BrdU (brown) and hematoxylin (purple). (E-J) 18- to 19-somite-stage embryos stained by in situ hybridization for *ccnb1*. The zic morphants show a reduction in *ccnb1* (F,H), primarily in the dorsal midbrain (between arrowheads in J). (E,F) Lateral views, anterior left. (G,H) Dorsal views, anterior left. (I,J) Representative cross-sections through midbrain.

narrow the onset of the proliferation defect in zic morphants to the stage between 16 and 18 somites.

To further characterize the cell-cycle defect in zic morphants, we analyzed cyclin gene expression by in situ hybridization. We were unable to detect a change in cyclinD1 (*ccnd1*) RNA, a G1 cyclin in morphants (not shown, *n*=50 controls and 56 morphants). CyclinB1 (*ccnb1*), a G2 cyclin, was consistently downregulated in morphants (Fig. 6E-J, *n*=49 controls and 77 morphants). Although this downregulation was not detectable by quantitative PCR analysis in whole embryos (supplementary material Fig. S5), a significant decrease in *ccnb1* staining was observed in the dorsal (Zic-expressing) portion of the midbrain in cross-sections (Fig. 6I,J). Together, our cell-cycle data show that there are fewer M- and S-phase cells in zic morphant midbrains by the 16- to 18-somite stage, and suggests that Zic proteins might regulate the cell cycle through activation of transcription of *ccnb1*, which is required for progression through the G2-M checkpoint.

Junction integrity, myosin II activity and DLHPs are independent of proliferation

We have established that zic gene expression is required for multiple cellular processes during midbrain neurulation, namely, apical actomyosin localization, junction integrity, and cell-cycle progression. Strikingly, all the observed morphant defects manifested at approximately the same stage: 16 somites. To test whether an initial proliferation defect could account for the disruption in junction integrity and/or actomyosin contraction, we exposed embryos to aphidicolin and hydroxyurea (A-H). These reagents block proliferation by preventing DNA replication (Gilman et al., 1980; Ikegami et al., 1978) and have been used effectively in zebrafish (Ciruna et al., 2006; Lowery and Sive, 2005; Lyons et al., 2005; Tawk et al., 2007). Embryos were treated with A-H or DMSO from 11- to 13-somite until 19- to 20-somite stages, then fixed and assayed for ZO-1 to indicate junction integrity or rMLC-*P* to assess actomyosin contraction. In addition, all embryos were labeled with anti-phosphohistone-H3, a marker of M-phase cells, to monitor the degree of cell-cycle inhibition. Although cell-cycle progression was effectively blocked (Fig. 7A,B, *n*=8), ZO-1 localization was normal in these embryos (Fig. 7C,D, *n*=8 controls, 8 A/H). rMLC-*P* distribution was also unaffected by A-H treatment (Fig. 7E,F, *n*=3 controls, 5 A/H). Furthermore, embryos treated with A-H for a longer period (10 somites to 24 hours) formed normally shaped ventricles (not shown, *n*=17) and DLHPs (Fig. 7G,H, *n*=5). Altogether, these data suggest that cell-cycle progression is not required for apical junction integrity, actomyosin contraction or DLHP formation. It is therefore unlikely that the proliferation reduction in zic morphants can account for the other defects.

Myosin II activity is necessary for junction integrity and cell-cycle progression

The data presented thus far suggest that Zic2a and Zic5 are required simultaneously for cell-cycle regulation and cytoskeletal organization. Alternatively, Zic proteins might act primarily in regulation of actomyosin contraction, which, in turn, could control proliferation and junction integrity. To determine whether the latter was a plausible scenario, we asked if blocking actomyosin contraction could affect apical junctions and/or cell proliferation in the neuroepithelium. Embryos were treated with blebbistatin or DMSO from the 12- to 14-somite stage until 20-somite stage, fixed and assayed for phosphohistone-H3 and ZO-1. DMSO controls showed several M-phase cells and normal ZO-1 distribution in the dorsal midbrain (Fig. 8A,C, *n*=7). By contrast, blebbistatin-treated embryos showed a severe reduction or absence of mitotic cells and abnormal ZO-1 distribution (Fig. 8B,D, *n*=6) reminiscent of that in zic morphants. These defects did not result from a simple developmental delay because blebbistatin-treated embryos analyzed later (23-somite stage) had the same phenotypes as younger embryos (not shown). Although these data do not exclude the possibility that Zic2a and Zic5 regulate proliferation and actomyosin contraction in parallel, they raise the intriguing possibility that their role in proliferation and junction integrity might be secondary to that in regulating the actomyosin network.

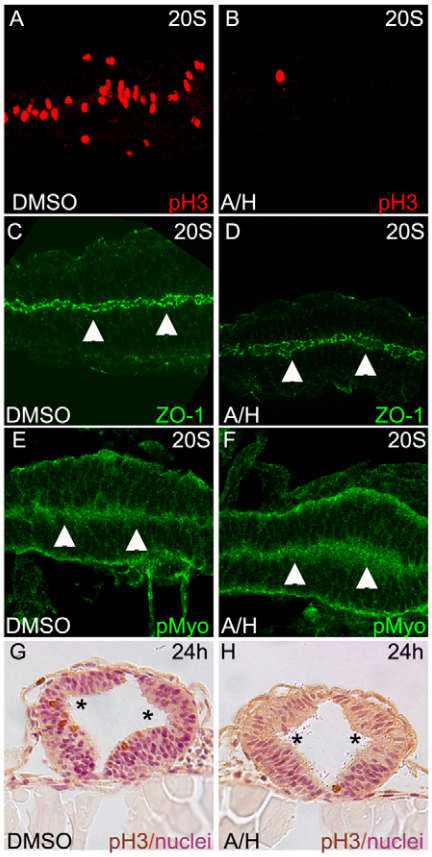

Fig. 7. Junction integrity, myosin activation and DLHP bending are normal in the absence of proliferation. (A-F) Immunostaining in horizontal confocal sections through dorsal midbrain at 20-somite stage. (A-B) Phosphohistone-H3 expression. C-D: ZO-1 expression. (E-F) rMLC-*P* expression. (G-H) The 24-hour midbrain cross-sections are labeled with phosphohistone-H3 (brown) and hematoxylin (purple). DMSO controls are shown on the left, aphidicolin-hydroxyurea treated embryos on the right. Asterisks indicate DLHPs. Arrowheads indicate the apical seam.

Canonical Wnt signaling is required for apical junction integrity and myosin II activity

zic2a and *zic5* are transcriptional targets of the canonical Wnt signaling pathway, a crucial regulator of midbrain growth (Nyholm et al., 2007). Although the relationship between Wnt signaling and actomyosin contraction has not been explored in vertebrate embryos, Wnt signaling is known to regulate actomyosin contraction during gastrulation in *C. elegans* (Lee et al., 2006). To test whether Wnt signaling is needed for apical actomyosin contraction, we used *hs:gfpΔtcf* transgenics to inhibit Tcf/Lef-mediated transcriptional

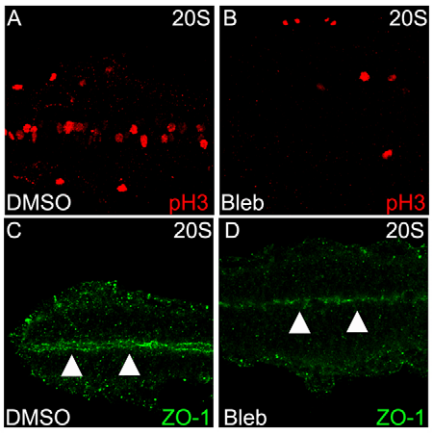

Fig. 8. Cell proliferation and junction integrity require active actomyosin contraction. (A-F) Immunostaining in horizontal confocal sections through dorsal midbrain at 20-somite stage. (A-B) Phosphohistone-H3 expression. (C-D) ZO-1 expression. DMSO controls are shown on the left, blebbistatin on the right. Arrowheads indicate the apical seam.

activation, the terminal event in the Wnt signaling cascade (Lewis et al., 2004). Upon heat-shock, *Tg(hs:gfpΔtcf)* embryos express GFPΔTcf, a fusion protein that cannot bind β-catenin and acts as a dominant repressor of Wnt target genes. *Tg(hs:gfpΔtcf)* embryos were heat-shocked at the 12-somite stage, allowed to recover and accumulate GFPΔTcf for 4 hours, and assayed for rMLC-*P* expression. Normal apical rMLC-*P* staining was seen in heat-shocked siblings lacking the transgene (Fig. 9A, *n*=6). Embryos expressing GFPΔTcf showed a reduction in apical rMLC-*P* (Fig. 9B, *n*=8) similar to that observed in zic morphants, demonstrating that intact Wnt signaling is required for apical myosin II activation.

Next, we asked whether Wnt signaling was required for apical junction integrity by assaying ZO-1 expression in *Tg(hs:gfpΔtcf)* embryos. Controls displayed the normal sub-apical ZO-1 localization (Fig. 9C, *n*=8), whereas *Tg(hs:gfpΔtcf)* showed patchy, discontinuous localization (Fig. 9D, *n*=12) reminiscent of the zic morphant phenotype. Subsequently, at 25 hpf, GFPΔTcf-expressing embryos failed to form DLHPs (Fig. 9E,F, *n*=4, 3 with small lumens, 1 with no lumen). Together, these data demonstrate a crucial role for canonical Wnt signaling in regulating apical myosin II, junction integrity and DLHP formation.

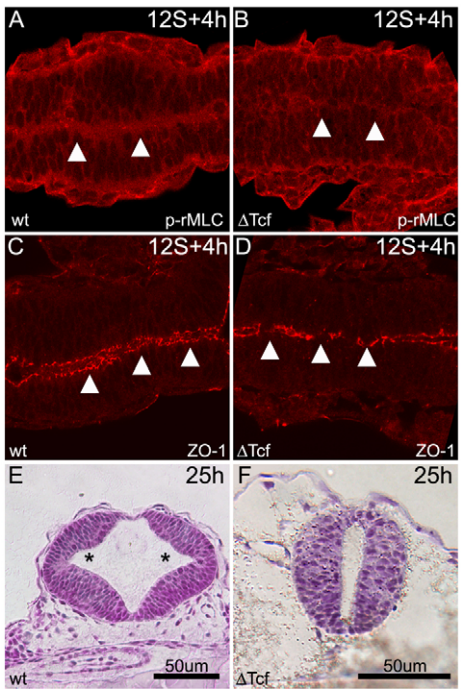

Fig. 9. Inhibition of Wnt signaling inhibits apical actomyosin contraction and disrupts apical junctions. (A-D) Immunostaining in horizontal confocal sections through dorsal midbrain at 21-somite stage. (A-B) rMLC-*P* expression. (C-D) ZO-1 expression. (E-F) 24 hpf midbrain cross-sections are labeled with hematoxylin (purple). All embryos were heat-shocked at 12-somite stage and recovered for 4 hours. Embryos carrying *Tg(hs:gfpΔtcf)* transgene are on the right, wild-type siblings on the left. Asterisks indicate DLHPs. Arrowheads mark the apical seam.

Discussion

Bending at hinge points, particularly at DLHPs, is required for cranial NT closure in mammals and birds. Although in zebrafish DLHPs form after the NT closes, we show that they are nonetheless important for morphogenesis and that their formation is controlled by conserved mechanisms. Using the zebrafish midbrain as a model, we present evidence that zic genes, which encode zinc-finger transcription factors, regulate apical actomyosin contraction and junction integrity, and are required for DLHP formation. Furthermore, we demonstrate a novel requirement for canonical Wnt signaling in regulating the cytoskeleton during DLHP morphogenesis. Our findings together with previously published data suggest that zic genes act downstream of Wnt signaling to simultaneously control proliferation and cytoskeletal organization during DLHP formation, and thus reveal a novel portion of the genetic network that regulates neurulation (Fig. 10).

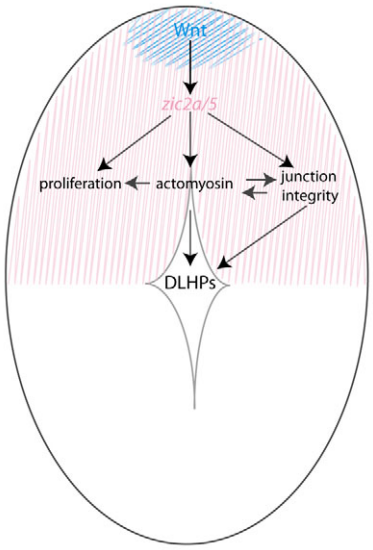

Fig. 10. A molecular model of *zic2a* and *zic5* in zebrafish DLHP development. Canonical Wnt signaling (blue) activates transcription of *zic2a* and *zic5* (pink). The resultant Zic proteins regulate the apical actomyosin network, apical junction integrity and proliferation in the dorsal midbrain. Wnt signaling might also have zic-independent roles in these cellular processes (Aruga et al., 2002; Ebert et al., 2003). Actomyosin contraction and apical junction integrity cooperate to cause DLHP bending, forming a diamond-shaped lumen. Proliferation is not required for DLHP bending.

zic genes, the cytoskeleton and DLHP formation

Several studies have observed that zic genes are required for NT morphogenesis (Aruga, 2004; Merzdorf, 2007), yet few have attempted to dissect the morphogenetic roles of these genes (Ybot-Gonzalez et al., 2007a). We found that DLHP bending depends on Zic function. This conclusion is supported by the failure of DLHP formation in Zic-depleted embryos, as well as by the striking correspondence between the normal zic gene expression pattern and DLHP location. Furthermore, analysis of actomyosin and junction marker distribution in Zic-knockdown embryos suggests that Zic proteins might control DLHP formation through regulation of the cytoskeleton. Although a direct interaction between Zic proteins and the cytoskeleton is conceivable, it is unlikely given their documented role as DNA-binding proteins and transcription factors (Mizugishi et al., 2001). Zic proteins probably regulate the cytoskeleton indirectly, through transcriptional regulation of target genes.

Although a concerted effort to identify direct Zic targets is in progress, several candidates are suggested by the recent literature, among them genes encoding Eph/ephrin signaling molecules. Eph/ephrin signaling has been shown to regulate adhesion and junctions in epithelial cells (Lee, H. S. et al., 2008; Pasquale, 2005). *EphB1* transcription is activated by Zic2 during retinal ganglion cell guidance in mouse (Lee, R. et al., 2008). Another group of potential Zic targets are genes that antagonize BMP signaling. In the mouse spinal cord, BMP signaling must be inhibited for DLHPs to form. This inhibition requires Zic2-induced expression of BMP antagonists (Ybot-Gonzalez et al., 2007a). It will be interesting to test whether the same genetic interaction operates in the cranial region, and to examine the relationship between BMP signaling levels and cytoskeletal organization.

We have not tested the function of zic genes in the zebrafish trunk, but studies in mice demonstrate that Zic genes are required for neurulation in both the brain and spinal cord (Aruga, 2004). However, pharmacological inhibition of actomyosin in the mouse embryo suggests that it is dispensable for spinal NT closure (Ybot-Gonzalez and Copp, 1999). Many mutations affecting actomyosin cause only cranial NTDs (Copp, 2005); yet Shroom, a regulator of apical actomyosin in the neuroepithelium and of DLHP formation, produces both cranial and spinal NTDs when disrupted (Hildebrand and Soriano, 1999), indicating that actomyosin might have a role in the trunk.

The localization of F-actin and active myosin in the apical neuroepithelium, combined with results from myosin II inhibition, suggest a role for an apical actomyosin network in DLHP development during zebrafish neurulation. A similar function of apical actomyosin has been documented in other organisms (Copp, 2005); however, it is unclear how this actomyosin network effects a bend in the neuroepithelium. There is evidence that localized apical actomyosin contraction can convert a subset of columnar epithelial cells into wedge-shaped cells, thus creating a hinge point (Haigo et al., 2003; Hildebrand, 2005); however, it remains to be determined whether this mechanism for tissue shape change occurs in zebrafish. It is unlikely that Zic proteins function locally at DLHPs to regulate actomyosin activity because the entire dorsal apical actomyosin network is disrupted upon knockdown of Zic2a and Zic5.

The apical actomyosin network may have a less direct role in DLHP bending through imparting rigidity at the apical neuroepithelial surface (Ybot-Gonzalez and Copp, 1999). Alternatively, the actomyosin network might regulate apical junction remodeling as it does in other systems (Bertet et al., 2004; Kishikawa et al., 2008; Miyake et al., 2006; Zallen and Wieschaus, 2004). Junction integrity would in turn affect cell-cell adhesion. A difference in adhesive properties between neighboring cells might be sufficient to allow bending, whereas other forces, for example tension from surrounding tissues or proton pumping, act to inflate the lumen. All of these possibilities are consistent with our findings that Zic transcription factors, which are expressed in a broad dorsal domain, control apical localization of F-actin and active myosin II, and that actomyosin contraction is required for localized DLHP bending. A possibility also exists that Zic-dependent myosin activity might effect changes at the basal cell surface or cause shortening along the apical-basal axis of the cells, which could lead to hinge-point formation.

Is cell-cycle regulation required for neurulation?

The neuroepithelium is highly proliferative during neurulation. However, results of our cell-cycle inhibition experiments suggest that major cellular processes required for NT morphogenesis, including DLHP bending, actomyosin contraction and apical junction maturation, can occur in the absence of proliferation. These results are consistent with previous studies in zebrafish and *Xenopus* demonstrating that neurulation proceeds normally when proliferation is inhibited (Ciruna et al., 2006; Harris and Hartenstein, 1991; Lowery and Sive, 2005). By contrast, exencephaly is strongly correlated with proliferation defects in the mouse (Gowen et al., 1996; Ishibashi et al., 1995; Sah et al., 1995; Zhong et al., 2000), and proliferation is differentially regulated along the D-V axis, with more proliferating cells dorsally. When this gradient is disrupted, as in *Phactr4* mutants, cytoskeletal organization remains normal, but DLHPs do not form (Kim et al., 2007).

In zebrafish, we observe slightly more S-phase cells dorsally than ventrally, and a reverse but equally subtle gradient when M-phase cells are labeled (Nyholm et al., 2007). In other words, unlike mouse embryos, zebrafish embryos do not appear to have a steep D-V proliferation gradient during neurulation. In A-H-treated embryos, the cell cycle is equally inhibited in dorsal and ventral regions, thereby eliminating any subtle gradient that might exist. These treated embryos form DLHPs normally, so if a proliferation gradient does exist in zebrafish, it is not required for DLHP formation. This finding highlights a divergence in the basic cellular mechanisms of neurulation in mammals and teleosts that needs to be analyzed further in other vertebrate models.

Multiple roles for Wnt signaling in neurulation

The non-canonical Wnt-PCP pathway has a well-documented role in epithelial morphogenesis, and in particular in shaping the neural tube (Kibar et al., 2007; Wang and Nathans, 2007). Studies in *Xenopus* suggest that PCP exerts its effect on NT closure by regulating cell-shape changes and apical constriction via Rho, a regulator of actomyosin contraction (Kinoshita et al., 2008). Having found a role for Zics in NT morphogenesis and actomyosin contraction, we thought it likely that Zics might be acting upstream of PCP. However, using two independent assays of the PCP pathway previously established in zebrafish, we found no evidence of PCP aberrations in Zic-depleted embryos.

Compared with the well-supported role of non-canonical Wnt signaling in neurulation, surprisingly little is known concerning the role of canonical Wnt signaling in neural tube morphogenesis. However, in *C. elegans*, Wnt-Frizzled signaling regulates morphogenetic movements during gastrulation by activating apical

actomyosin contraction through phosphorylation of myosin II (Lee et al., 2006). Here, we provide evidence that in vertebrate embryos Wnt signaling is also required upstream of myosin II phosphorylation, as well as for DLHP formation. This morphogenetic role for Wnt proteins appears to be independent of their previously documented mitogenic role (Ikeya et al., 1997; Panhuysen et al., 2004), because proliferation is dispensable for actomyosin contraction, junction integrity and DLHP formation. We thereby document a new role for Wnt signaling in regulating actomyosin contraction during vertebrate morphogenesis.

From pattern to morphology: a role for Zic transcription factors in DLHP bending during neurulation

Although neural pattern formation is well understood, and the mechanistic details of coordinated cell shape changes during epithelial morphogenesis are under intense scrutiny, we know relatively little of how gene expression patterns bring about coordinated shape changes (Chanut-Delalande et al., 2006). *zic2a* and *zic5* expression is patterned by Wnt signaling and possibly other signaling pathways. This pattern precisely predicts the future location of DLHPs, a conserved shape change in NT morphogenesis. This specific colocalization argues that Zic protein function is proximal to the cytoskeletal changes that underlie DLHP formation, i.e. that they are key players in coordinating pattern and morphogenesis. Identification of direct Zic protein targets, probably important regulators of actomyosin contraction, apical junction formation or both, will yield important mechanistic insights into the role of cytoskeletal regulation during vertebrate neurulation.

Materials and Methods

Zebrafish strains and embryo manipulation

Adult zebrafish were maintained according to established methods (Westerfield, 1995). Embryos were obtained from natural matings and staged (Kimmel et al., 1995). The following transgenic lines were used: *Tg(pBOS:H2Bgfp)* (Jesuthasan and Subburaju, 2002), *Tg(zic2a-D5:egfp)* (Nyholm et al., 2007) and *Tg(hs:gfpΔtcf)* (Lewis et al., 2004). Heterozygous *Tg(hs:gfpΔtcf)* embryos were heat-shocked at 37°C for 45 minutes, then recovered at 29°C and fixed for immunostaining. *zic2a* and *zic5* splice-blocking (1 ng/nl each), Zic2a and Zic5 translation-blocking (6.6 ng/nl) or standard control (7-8 ng/nl) MOs (Gene Tools) were diluted in 1× Danieau buffer and 0.5-1 nl was injected at the 1- to 2-cell stage (Nyholm et al., 2007).

Blebbistatin treatments

(±)Blebbistatin (active) and *R*-(+)Blebbistatin (inactive, Tocris Biosciences) were dissolved in DMSO to make a 10 mM stock solution. Dechorionated 15- to 16-somite-stage embryos were soaked in 1:100 dilution of stocks or in 1% DMSO/E3 (carrier control) at 29°C and fixed at the appropriate stage for histological and/or immunological analysis.

In situ hybridization and histology

Anti-sense RNA probes were transcribed from plasmid templates: *zic2a* (Grinblat and Sive, 2001), *zic5* (Toyama et al., 2004), *ccnD1* and *ccnb1* (Thisse et al., 2001). In situ hybridization was performed as previously described (Gillhouse et al., 2004). Stained embryos were embedded in Eponate 12 medium (Ted Pella), and 5 μm sections were cut with a steel blade on an American Optical Company microtome. Nuclei were counterstained with Mayer's hematoxylin.

Immunohistochemistry

Embryos were fixed in 4% formaldehyde in PBS for staining with the following primary antibodies: anti-pH3 (Upstate Biotechnology, 1:500), anti-β-catenin (Sigma, 1:1000), anti-ZO-1 (Zymed, 1:200), anti-Mpp5a (1:50). Embryos were fixed in 0.25% glutaraldehyde, 4% formaldehyde with 5 mM EGTA and 0.2% Triton X-100 for staining with anti-rMLC-*P* [Cell Signaling (Theusch et al., 2006); 1:50]. Glutaraldehyde was quenched with 100 mM sodium borohydride before applying antibody. Primary antibodies were detected fluorescently with Alexa-Fluor-conjugated goat anti-rabbit or anti-mouse secondary antibodies (Molecular Probes, 1:500) or with Vectastain Elite ABC kit (Vector Laboratories). F-actin was labeled with either Alexa Fluor 488-phalloidin or Alexa Fluor 568-phalloidin (Molecular Probes, 1:100) for 2 hours at room temperature in PBS with Triton X-100. Embryos were mounted in methyl cellulose and horizontal sections were taken on an Olympus IX81 inverted microscope with Fluoview 1000 confocal package. For cross-sections, embryos were embedded in 4% agarose. Vibratome sections were cut at 60 μm, mounted in methyl cellulose, and imaged by confocal microscopy.

Apical F-actin quantification

Using ImageJ, a region of interest (ROI) two-thirds the width of the neural tube and ~80 μm long was positioned over each image such that it was bisected along its length by the apical seam. Background threshold was defined as the mode pixel intensity within this ROI. To measure apical F-actin signal, a second ROI one-third the width of the neural tube was positioned to include only apical regions. Within this second ROI, total relative apical F-actin signal was then computed as the sum of all pixel intensities above threshold divided by the threshold value. Total relative signal was normalized to the ROI area, yielding the total relative signal density that should be proportional to apical F-actin concentration. Morphant and control groups were compared using the Student's *t*-test.

Live imaging

Tg(pBOS:H2Bgfp) embryos were injected with ~20 pg sense RNA encoding mCherry-Utr-CH (Burkel et al., 2007) at the one-cell stage, followed by an injection with control or zic MO at the 1- to 2-cell stage. Embryos were raised to the 13-somite stage and mounted in 1% LMP agarose in Grinzberg's Ringers with tricaine. Confocal images of a single *Z*-plane through the dorsal midbrain were taken every minute for 2.5-3 hours at 60× magnification. Collections of images were made into movies using ImageJ software (NIH).

PCP analysis

Tg(pBOS:H2BGfp) embryos were injected with control or zic MOs at 1-cell stage, fixed at 19-somites, and stained with Alexa Fluor 568-phalloidin. Horizontal confocal *Z*-sections were taken at 1 μm intervals through the dorsal half of the midbrain. *pBOS:H2Bgfp* labeled condensed chromatin and was used to estimate the location of the mitotic spindle in M-phase cells. Phalloidin marked the midline of the neuroepithelium. Image files were scored blindly in ImageJ by measuring the angle of the spindle relative to the midline. GFP-Prickle (GFP-Pk) labeling was previously described (Ciruna et al., 2006). 25 pg GFP-Pk RNA was injected into control or zic morphants at the 8-cell stage and GFP-Pk localization was examined at 12-somite stage. This scatter labeling method produced mosaic GFP-Pk-expressing embryos, so individual neuroepithelial cells could be scored. Expressing cells were scored for cytoplasmic versus punctate expression and cells with punctate expression were further analyzed for an anterior, lateral or posterior bias in expression.

Cell-cycle studies

Bromodeoxyuridine (BrdU) labeling was performed as described (Shepard et al., 2004) with the following modifications: BrdU was incorporated into 18-somite-stage embryos for 4 minutes at 29°C. Following fixation, embryos were treated with proteinase-K for 5 minutes and postfixed for 15 minutes in 4% formaldyhyde; anti-BrdU (Roche, 1:100) was detected with Vectastain Elite ABC kit (Vector Laboratories) using DAB (Sigma) substrate. Cross-sections of BrdU-labeled embryos were counterstained with hematoxylin, and the number of BrdU-positive cells and total cells were counted in dorsal, middle and ventral regions of each section. To define these regions, the total height of each midbrain cross-section was measured and then the section was divided into equal thirds. At 16-somite stage 25 sections from five morphants and two sections from four controls were analyzed. At 18-somite stage, 37 sections from eight morphants and 30 sections from six controls were analyzed. A *t*-test and ANOVA (SigmaPlot) were used to compare the percent of BrdU-positive cells in morphant and control embryos. Treatments with aphidicolin and hydroxyurea was essentially as described (Ciruna et al., 2006, Tawk et al., 2007). Aphidicolin (Sigma) was dissolved in DMSO to make 15 mM stock solution. Hydroxyurea was dissolved in water to make 2 M stock. 10- to 13-somite-stage embryos were soaked in a 1:100 dilution of stocks in E3 or in 1% DMSO-E3 (carrier control) at 29°C and fixed at the appropriate stage for histological and/or immunological analysis. Anti-phosphorylated histone H3 was used to label M-phase cells, as described previously (Nyholm et al., 2007).

We thank Jason Berndt, Mary Halloran, Brian Burkel, Bill Bement, Francisco Pelegri and the Zebrafish International Resource Center for sharing antibodies, plasmids and zebrafish lines, and Jim Pawley, Tony Stretton, Grace Lee and John Fallon for sharing equipment. We are grateful to Nick Sanek, Aaron Taylor and Jessica Pierson for valuable discussions throughout the course of this work, to Aaron Taylor for help with F-actin quantification and qPCR anaylsis, to Bill Feeny for help with illustrations, and to Laura Sherrill for expert technical help. This work was funded by an NIH RO1 grant to Y.G. Deposited in PMC for release after 12 months.

References

Aaku-Saraste, E., Hellwig, A. and Huttner, W. B. (1996). Loss of occludin and functional tight junctions, but not ZO-1, during neural tube closure-remodeling of the neuroepithelium prior to neurogenesis. *Dev. Biol.* **180**, 664-679.

Aruga, J. (2004). The role of Zic genes in neural development. *Mol. Cell Neurosci.* **26**, 205-221.

Aruga, J., Nagai, T., Tokuyama, T., Hayashizaki, Y., Okazaki, Y., Chapman, V. M. and Mikoshiba, K. (1996). The mouse zic gene family: homologues of the Drosophila pair-rule gene odd-paired. *J. Biol. Chem.* **271**, 1043-1047.

Aruga, J., Inoue, T., Hoshino, J. and Mikoshiba, K. (2002). Zic2 controls cerebellar development in cooperation with Zic1. *J. Neurosci.* **22**, 218-225.

Bertet, C., Sulak, L. and Lecuit, T. (2004). Myosin-dependent junction remodelling controls planar cell intercalation and axis elongation. *Nature* **429**, 667-671.

Bit-Avragim, N., Hellwig, N., Rudolph, F., Munson, C., Stainier, D. Y. and Abdelilah-Seyfried, S. (2008). Divergent polarization mechanisms during vertebrate epithelial development mediated by the Crumbs complex protein Nagie oko. *J. Cell Sci.* **121**, 2503-2510.

Brembeck, F. H., Rosario, M. and Birchmeier, W. (2006). Balancing cell adhesion and Wnt signaling, the key role of beta-catenin. *Curr. Opin. Genet. Dev.* **16**, 51-59.

Brewster, R., Lee, J. and Ruiz i Altaba, A. (1998). Gli/Zic factors pattern the neural plate by defining domains of cell differentiation. *Nature* **393**, 579-583.

Brouns, M. R., Matheson, S. F., Hu, K. Q., Delalle, I., Caviness, V. S., Silver, J., Bronson, R. T. and Settleman, J. (2000). The adhesion signaling molecule p190 RhoGAP is required for morphogenetic processes in neural development. *Development* **127**, 4891-4903.

Burkel, B. M., von Dassow, G. and Bement, W. M. (2007). Versatile fluorescent probes for actin filaments based on the actin-binding domain of utrophin. *Cell Motil. Cytoskeleton* **64**, 822-832.

Chanut-Delalande, H., Fernandes, I., Roch, F., Payre, F. and Plaza, S. (2006). Shavenbaby couples patterning to epidermal cell shape control. *PLoS Biol.* **4**, e290.

Ciruna, B., Jenny, A., Lee, D., Mlodzik, M. and Schier, A. F. (2006). Planar cell polarity signalling couples cell division and morphogenesis during neurulation. *Nature* **439**, 220-224.

Colas, J. F. and Schoenwolf, G. C. (2001). Towards a cellular and molecular understanding of neurulation. *Dev. Dyn.* **221**, 117-145.

Copp, A. J. (2005). Neurulation in the cranial region-normal and abnormal. *J. Anat.* **207**, 623-635.

Copp, A. J., Greene, N. D. and Murdoch, J. N. (2003). The genetic basis of mammalian neurulation. *Nat. Rev. Genet.* **4**, 784-793.

Curtin, J. A., Quint, E., Tsipouri, V., Arkell, R. M., Cattanach, B., Copp, A. J., Henderson, D. J., Spurr, N., Stanier, P., Fisher, E. M. et al. (2003). Mutation of Celsr1 disrupts planar polarity of inner ear hair cells and causes severe neural tube defects in the mouse. *Curr. Biol.* **13**, 1129-1133.

Ebert, P. J., Timmer, J. R., Nakada, Y., Helms, A. W., Parab, P. B., Liu, Y., Hunsaker, T. L. and Johnson, J. E. (2003). Zic1 represses Math1 expression via interactions with the Math1 enhancer and modulation of Math1 autoregulation. *Development* **130**, 1949-1959.

Elms, P., Siggers, P., Napper, D., Greenfield, A. and Arkell, R. (2003). Zic2 is required for neural crest formation and hindbrain patterning during mouse development. *Dev. Biol.* **264**, 391-406.

Geldmacher-Voss, B., Reugels, A. M., Pauls, S. and Campos-Ortega, J. A. (2003). A 90-degree rotation of the mitotic spindle changes the orientation of mitoses of zebrafish neuroepithelial cells. *Development* **130**, 3767-3780.

Gillhouse, M., Wagner Nyholm, M., Hikasa, H., Sokol, S. Y. and Grinblat, Y. (2004). Two Frodo/Dapper homologs are expressed in the developing brain and mesoderm of zebrafish. *Dev. Dyn.* **230**, 403-409.

Gilman, A. F., Goodman, L. S. and Gilman, A. (1980). *The Pharmacological Basis of Therapeutics*. New York: Macmillan.

Gong, Y., Mo, C. and Fraser, S. E. (2004). Planar cell polarity signalling controls cell division orientation during zebrafish gastrulation. *Nature* **430**, 689-693.

Gowen, L. C., Johnson, B. L., Latour, A. M., Sulik, K. K. and Koller, B. H. (1996). Brca1 deficiency results in early embryonic lethality characterized by neuroepithelial abnormalities. *Nat. Genet.* **12**, 191-194.

Grinberg, I. and Millen, K. J. (2005). The ZIC gene family in development and disease. *Clin. Genet.* **67**, 290-296.

Grinblat, Y. and Sive, H. (2001). zic Gene expression marks anteroposterior pattern in the presumptive neurectoderm of the zebrafish gastrula. *Dev. Dyn.* **222**, 688-693.

Haigo, S. L., Hildebrand, J. D., Harland, R. M. and Wallingford, J. B. (2003). Shroom induces apical constriction and is required for hingepoint formation during neural tube closure. *Curr. Biol.* **13**, 2125-2137.

Harris, W. A. and Hartenstein, V. (1991). Neuronal determination without cell division in Xenopus embryos. *Neuron* **6**, 499-515.

Hildebrand, J. D. (2005). Shroom regulates epithelial cell shape via the apical positioning of an actomyosin network. *J. Cell Sci.* **118**, 5191-5203.

Hildebrand, J. D. and Soriano, P. (1999). Shroom, a PDZ domain-containing actin-binding protein, is required for neural tube morphogenesis in mice. *Cell* **99**, 485-497.

Hong, E. and Brewster, R. (2006). N-cadherin is required for the polarized cell behaviors that drive neurulation in the zebrafish. *Development* **133**, 3895-3905.

Ikegami, S., Taguchi, T., Ohashi, M., Oguro, M., Nagano, H. and Mano, Y. (1978). Aphidicolin prevents mitotic cell division by interfering with the activity of DNA polymerase-alpha. *Nature* **275**, 458-460.

Ikeya, M., Lee, S. M., Johnson, J. E., McMahon, A. P. and Takada, S. (1997). Wnt signalling required for expansion of neural crest and CNS progenitors. *Nature* **389**, 966-970.

Inoue, T., Hatayama, M., Tohmonda, T., Itohara, S., Aruga, J. and Mikoshiba, K. (2004). Mouse Zic5 deficiency results in neural tube defects and hypoplasia of cephalic neural crest derivatives. *Dev. Biol.* **270**, 146-162.

Ishibashi, M., Ang, S. L., Shiota, K., Nakanishi, S., Kageyama, R. and Guillemot, F. (1995). Targeted disruption of mammalian hairy and Enhancer of split homolog-1 (HES-1) leads to up-regulation of neural helix-loop-helix factors, premature neurogenesis, and severe neural tube defects. *Genes Dev.* **9**, 3136-3148.

Itoh, M., Nagafuchi, A., Yonemura, S., Kitani-Yasuda, T., Tsukita, S. and Tsukita, S. (1993). The 220-kD protein colocalizing with cadherins in non-epithelial cells is identical to ZO-1, a tight junction-associated protein in epithelial cells: cDNA cloning and immunoelectron microscopy. *J. Cell Biol.* **121**, 491-502.

Jessen, J. R., Topczewski, J., Bingham, S., Sepich, D. S., Marlow, F., Chandrasekhar, A. and Solnica-Krezel, L. (2002). Zebrafish trilobite identifies new roles for Strabismus in gastrulation and neuronal movements. *Nat. Cell Biol.* **4**, 610-615.

Jesuthasan, S. and Subburaju, S. (2002). Gene transfer into zebrafish by sperm nuclear transplantation. *Dev. Biol.* **242**, 88-95.

Kibar, Z., Capra, V. and Gros, P. (2007). Toward understanding the genetic basis of neural tube defects. *Clin. Genet.* **71**, 295-310.

Kim, T. H., Goodman, J., Anderson, K. V. and Niswander, L. (2007). Phactr4 regulates neural tube and optic fissure closure by controlling PP1-, Rb-, and E2F1-regulated cell-cycle progression. *Dev. Cell* **13**, 87-102.

Kimmel, C. B., Ballard, W. W., Kimmel, S. R., Ullman, B. and Schilling, T. F. (1995). Stages of embryonic development of the zebrafish. *Dev. Dyn.* **203**, 253-310.

Kinoshita, N., Sasai, N., Misaki, K. and Yonemura, S. (2008). Apical accumulation of rho in the neural plate is important for neural plate cell shape change and neural tube formation. *Mol. Biol. Cell* **19**, 2289-2299.

Kishikawa, M., Suzuki, A. and Ohno, S. (2008). aPKC enables development of zonula adherens by antagonizing centripetal contraction of the circumferential actomyosin cables. *J. Cell Sci.* **121**, 2481-2492.

Koppen, M., Fernandez, B. G., Carvalho, L., Jacinto, A. and Heisenberg, C. P. (2006). Coordinated cell-shape changes control epithelial movement in zebrafish and Drosophila. *Development* **133**, 2671-2681.

Kovacs, M., Toth, J., Hetenyi, C., Malnasi-Csizmadia, A. and Sellers, J. R. (2004). Mechanism of blebbistatin inhibition of myosin II. *J. Biol. Chem.* **279**, 35557-35563.

Lanier, L. M., Gates, M. A., Witke, W., Menzies, A. S., Wehman, A. M., Macklis, J. D., Kwiatkowski, D., Soriano, P. and Gertler, F. B. (1999). Mena is required for neurulation and commissure formation. *Neuron* **22**, 313-325.

Lee, C., Scherr, H. M. and Wallingford, J. B. (2007). Shroom family proteins regulate gamma-tubulin distribution and microtubule architecture during epithelial cell shape change. *Development* **134**, 1431-1441.

Lee, H. S., Nishanian, T. G., Mood, K., Bong, Y. S. and Daar, I. O. (2008). EphrinB1 controls cell-cell junctions through the Par polarity complex. *Nat. Cell Biol.* **10**, 979-986.

Lee, J. Y., Marston, D. J., Walston, T., Hardin, J., Halberstadt, A. and Goldstein, B. (2006). Wnt/Frizzled signaling controls C. elegans gastrulation by activating actomyosin contractility. *Curr. Biol.* **16**, 1986-1997.

Lee, R., Petros, T. J. and Mason, C. A. (2008). Zic2 regulates retinal ganglion cell axon avoidance of ephrinB2 through inducing expression of the guidance receptor EphB1. *J. Neurosci.* **28**, 5910-5919.

Lewis, J. L., Bonner, J., Modrell, M., Ragland, J. W., Moon, R. T., Dorsky, R. I. and Raible, D. W. (2004). Reiterated Wnt signaling during zebrafish neural crest development. *Development* **131**, 1299-1308.

Lowery, L. A. and Sive, H. (2005). Initial formation of zebrafish brain ventricles occurs independently of circulation and requires the nagie oko and snakehead/atp1a1a.1 gene products. *Development* **132**, 2057-2067.

Lyons, D. A., Pogoda, H. M., Voas, M. G., Woods, I. G., Diamond, B., Nix, R., Arana, N., Jacobs, J. and Talbot, W. S. (2005). erbb3 and erbb2 are essential for schwann cell migration and myelination in zebrafish. *Curr. Biol.* **15**, 513-524.

Menzies, A. S., Aszodi, A., Williams, S. E., Pfeifer, A., Wehman, A. M., Goh, K. L., Mason, C. A., Fassler, R. and Gertler, F. B. (2004). Mena and vasodilator-stimulated phosphoprotein are required for multiple actin-dependent processes that shape the vertebrate nervous system. *J. Neurosci.* **24**, 8029-8038.

Merzdorf, C. S. (2007). Emerging roles for zic genes in early development. *Dev. Dyn.* **236**, 922-940.

Miyake, Y., Inoue, N., Nishimura, K., Kinoshita, N., Hosoya, H. and Yonemura, S. (2006). Actomyosin tension is required for correct recruitment of adherens junction components and zonula occludens formation. *Exp. Cell Res.* **312**, 1637-1650.

Mizugishi, K., Aruga, J., Nakata, K. and Mikoshiba, K. (2001). Molecular properties of Zic proteins as transcriptional regulators and their relationship to GLI proteins. *J. Biol. Chem.* **276**, 2180-2188.

Morriss-Kay, G. and Tuckett, F. (1985). The role of microfilaments in cranial neurulation in rat embryos: effects of short-term exposure to cytochalasin D. *J. Embryol. Exp. Morphol.* **88**, 333-348.

Morriss-Kay, G., Wood, H. and Chen, W. H. (1994). Normal neurulation in mammals. *Ciba Found. Symp.* **181**, 51-63; discussion 63-69.

Nagai, T., Aruga, J., Takada, S., Gunther, T., Sporle, R., Schughart, K. and Mikoshiba, K. (1997). The expression of the mouse Zic1, Zic2, and Zic3 gene suggests an essential role for Zic genes in body pattern formation. *Dev. Biol.* **182**, 299-313.

Nyholm, M. K., Wu, S. F., Dorsky, R. I. and Grinblat, Y. (2007). The zebrafish zic2a-zic5 gene pair acts downstream of canonical Wnt signaling to control cell proliferation in the developing tectum. *Development* **134**, 735-746.

Panhuysen, M., Vogt Weisenhorn, D. M., Blanquet, V., Brodski, C., Heinzmann, U., Beisker, W. and Wurst, W. (2004). Effects of Wnt1 signaling on proliferation in the developing mid-/hindbrain region. *Mol. Cell Neurosci.* **26**, 101-111.

Pasquale, E. B. (2005). Eph receptor signalling casts a wide net on cell behaviour. *Nat. Rev. Mol. Cell. Biol.* **6**, 462-475.
Roffers-Agarwal, J., Xanthos, J. B., Kragtorp, K. A. and Miller, J. R. (2008). Enabled (Xena) regulates neural plate morphogenesis, apical constriction, and cellular adhesion required for neural tube closure in Xenopus. *Dev. Biol.* **314**, 393-403.
Sadler, T. W., Greenberg, D., Coughlin, P. and Lessard, J. L. (1982). Actin distribution patterns in the mouse neural tube during neurulation. *Science* **215**, 172-174.
Sah, V. P., Attardi, L. D., Mulligan, G. J., Williams, B. O., Bronson, R. T. and Jacks, T. (1995). A subset of p53-deficient embryos exhibit exencephaly. *Nat. Genet.* **10**, 175-180.
Schoenwolf, G. C., Folsom, D. and Moe, A. (1988). A reexamination of the role of microfilaments in neurulation in the chick embryo. *Anat. Rec.* **220**, 87-102.
Shepard, J. L., Stern, H. M., Pfaff, K. L. and Amatruda, J. F. (2004). Analysis of the cell cycle in zebrafish embryos. *Methods Cell Biol.* **76**, 109-125.
Smith, J. L. and Schoenwolf, G. C. (1997). Neurulation: coming to closure. *Trends Neurosci.* **20**, 510-517.
Somlyo, A. P. and Somlyo, A. V. (2003). Ca^{2+} sensitivity of smooth muscle and nonmuscle myosin II: modulated by G proteins, kinases, and myosin phosphatase. *Physiol. Rev.* **83**, 1325-1358.
Tawk, M., Araya, C., Lyons, D. A., Reugels, A. M., Girdler, G. C., Bayley, P. R., Hyde, D. R., Tada, M. and Clarke, J. D. (2007). A mirror-symmetric cell division that orchestrates neuroepithelial morphogenesis. *Nature* **446**, 797-800.
Tepass, U., Truong, K., Godt, D., Ikura, M. and Peifer, M. (2000). Cadherins in embryonic and neural morphogenesis. *Nat. Rev. Mol. Cell. Biol.* **1**, 91-100.
Thisse, B., Pflumio, S., Furthauer, M., Loppin, B., Heyer, V., Degrave, A., Woehl, R., Luz, A., Steffan, T., Charbonnier, X. Q. et al. (2001). Expression of the zebrafish genome during embryogenesis (NIH RO1 RR15402). In *ZFIN Direct Data Submission*.
Toyama, R., Gomez, D. M., Mana, M. D. and Dawid, I. B. (2004). Sequence relationships and expression patterns of zebrafish zic2 and zic5 genes. *Gene Expr. Patterns* **4**, 345-350.
van Straaten, H. W., Sieben, I. and Hekking, J. W. (2002). Multistep role for actin in initial closure of the mesencephalic neural groove in the chick embryo. *Dev. Dyn.* **224**, 103-108.
Veeman, M. T., Slusarski, D. C., Kaykas, A., Louie, S. H. and Moon, R. T. (2003). Zebrafish prickle, a modulator of noncanonical Wnt/Fz signaling, regulates gastrulation movements. *Curr. Biol.* **13**, 680-685.
Wang, J., Hamblet, N. S., Mark, S., Dickinson, M. E., Brinkman, B. C., Segil, N., Fraser, S. E., Chen, P., Wallingford, J. B. and Wynshaw-Boris, A. (2006). Dishevelled genes mediate a conserved mammalian PCP pathway to regulate convergent extension during neurulation. *Development* **133**, 1767-1778.
Wang, Y. and Nathans, J. (2007). Tissue/planar cell polarity in vertebrates: new insights and new questions. *Development* **134**, 647-658.
Wei, X. and Malicki, J. (2002). nagie oko, encoding a MAGUK-family protein, is essential for cellular patterning of the retina. *Nat. Genet.* **31**, 150-157.
Westerfield, M. (1995). *The Zebrafish Book*. Eugene, OR: University of Oregon Press.
Xu, W., Baribault, H. and Adamson, E. D. (1998). Vinculin knockout results in heart and brain defects during embryonic development. *Development* **125**, 327-337.
Yamamoto, S., Nishimura, O., Misaki, K., Nishita, M., Minami, Y., Yonemura, S., Tarui, H. and Sasaki, H. (2008). Cthrc1 selectively activates the planar cell polarity pathway of Wnt signaling by stabilizing the Wnt-receptor complex. *Dev. Cell* **15**, 23-36.
Ybot-Gonzalez, P. and Copp, A. J. (1999). Bending of the neural plate during mouse spinal neurulation is independent of actin microfilaments. *Dev. Dyn.* **215**, 273-283.
Ybot-Gonzalez, P., Gaston-Massuet, C., Girdler, G., Klingensmith, J., Arkell, R., Greene, N. D. and Copp, A. J. (2007a). Neural plate morphogenesis during mouse neurulation is regulated by antagonism of Bmp signalling. *Development* **134**, 3203-3211.
Ybot-Gonzalez, P., Savery, D., Gerrelli, D., Signore, M., Mitchell, C. E., Faux, C. H., Greene, N. D. and Copp, A. J. (2007b). Convergent extension, planar-cell-polarity signalling and initiation of mouse neural tube closure. *Development* **134**, 789-799.
Zallen, J. A. and Wieschaus, E. (2004). Patterned gene expression directs bipolar planar polarity in Drosophila. *Dev. Cell* **6**, 343-355.
Zhong, W., Jiang, M. M., Schonemann, M. D., Meneses, J. J., Pedersen, R. A., Jan, L. Y. and Jan, Y. N. (2000). Mouse numb is an essential gene involved in cortical neurogenesis. *Proc. Natl. Acad. Sci. USA* **97**, 6844-6849.